ce/papers
The online collection for conference papers in civil engineering
Ernst & Sohn A Wiley Brand

ORIGINAL ARTICLE

SDSS 2022
The International Colloquium on Stability and Ductility of Steel Structures
14-16 September, University of Aveiro, Portugal
Ernst & Sohn A Wiley Brand

Influence of the Shape of Initial Imperfections on Single Web and Flange Steel Plates at Elevated Temperatures

Luca Possidente[1], Nicola Tondini[1]

Correspondence

Dr. Luca Possidente
University of Trento
Department of Civil, Environmental and Mechanical Engineering
Via Mesiano 77
38123 Trento
Email: luca.possidente@unitn.it

Abstract

In the last decades the buckling of steel members in fire has attracted the attention of the scientific community, but considerations about the choice of the initial imperfections have been rarely the focus of scientific publications. However, initial imperfections play a primary role in the definition of the resistance, especially when local buckling is investigated. Although the lowest buckling mode is usually employed, the definition of an appropriate imperfection shape providing, for instance, the lowest resistance is not straightforward. Even more so when the local behaviour at elevated temperatures is being studied, since the buckling behaviour may differ from the one at ambient temperature, owing to the steel degradation and possible load redistributions. In this paper steel plates in compression at elevated temperatures are studied considering different shapes of imperfection. A parametric analysis on webs and flanges composing Class 4 HE and IPE sections with S355 steel grade is presented, considering five temperatures in a relevant range (400-800°C) and several plate aspect ratios. The influence of the imperfection shapes on the resistance depending on the temperature, the length and the slenderness of the web and flange plates is discussed.

Keywords

Steel members, fire behaviour, steel plates, Class 4 sections, local buckling

1 Introduction

Buckling of steel members is one of the major concerns in the design of steel structures. Design solutions are usually adopted to avoid global buckling, but also local effects need to be carefully considered. Indeed, in steel sections composed of very slender plates, e.g., Class 4 sections according to EN 1993-1-1 [1], local buckling prevents from attaining the full sectional capacity. For this reason, EN 1993-1-1 [1] and EN 1993-1-5 [2] provide indications to account for the effect of local buckling of steel sections, e.g., H or I sections, based on simple considerations on the buckling of the single plates of which the sections are composed of, e.g., webs and flanges. This approach is extended to the design in fire situation, in which sections sensitive to local buckling are identified by accounting for the degradation of the mechanical properties of steel [3]. However, due to the non-linear behaviour, the properties degradation and the possible load redistributions that may appear at elevated temperature, the behaviour of steel members in fire may differ from the one at ambient temperature and local buckling phenomena should be investigated carefully.

Detailed investigations on the buckling behaviour of steel elements are usually carried out by means of numerical simulation. The typical procedure employed in the numerical analyses implies the introduction of initial geometrical imperfections in the numerical models, though procedures that do not require the definition of initial imperfections can be found in the literature [4],[5]. More imperfections with different shapes are sometimes combined, in particular when both local and global buckling are investigated, to maximise the unfavourable effects. The shape of the imperfections is usually based on a preliminary linear buckling analysis LBA, which provides the shape of the lowest buckling mode, while the amplitude of the imperfections is defined as fractions of the member or plate length, e.g., ℓ/1000, b/100 or h/100, or according to provisions from different standards [6]-[8].

The studies on which the EN 1993-1-2 [3] relies for the provisions on the global buckling of steel members in fire were available already in the late 90's [9],[10], but only recently researchers focused on the numerical simulation of local buckling [11]-[18] or local-global buckling interaction [19]-[22] in steel members at elevated temperature. Aiming to provide conservative provisions applicable in the design process, mainly imperfections shapes that should provide the lowest failure loads were used, i.e., shapes from LBA, rather than shapes representative of actual imperfections in steel elements. Though several researchers focused on the consequences of the choice of the magnitude of the initial imperfection [15],[19],[22], only in few works the buckling resistance of steel elements at elevated temperature was investigated considering different shapes of imperfection [16],[19],[22]. Furthermore, extensive numerical studies comparing the resistance obtained with LBA-based shapes with the ones

1. University of Trento, Trento, Italy.

Open Access Funding provided by Universita degli Studi di Trento within the CRUI-CARE Agreement.

Correction added on November 25, 2022, after first online publication: CRUI-CARE funding statement has been added.

obtained with other shapes of imperfections are not available, and only a brief discussion on the influence of the shape of imperfections on the resistance of compressed steel plates was presented in [16].

This paper presents an extensive parametric analysis of compressed steel plates composing commercial HE and IPE sections at elevated temperatures considering different shapes of imperfection. Indications on the shapes of imperfections entailing the lowest compressive loads are provided for S355 Class 4 sections at elevated temperatures, depending on the temperature, the length and the slenderness of the studied web and flange plates.

2 Numerical simulation

A parametric analysis was conducted on plates with a uniform temperature distribution, uniform compressive stress and S355 steel grade representing webs and flanges composing commercial HE and IPE sections. Web and flange plates belonging to the sections listed in Table 1 were studied. All plates correspond to Class 4 sections only, in order to focus on sections particularly sensitive to local buckling. Sections were classified for a S355 steel grade according to the classification at elevated temperature

$$\varepsilon_\theta = 0.85\sqrt{\frac{235}{f_y}} \quad (1)$$

Where f_y is the steel yield strength expressed in MPa.

Table 1 Investigated steel webs and flanges

Section		web		flange	
	r [mm]	h [mm]	t_w [mm]	b [mm]	t_f [mm]
HE 200 AA	18	186	5.5	200	8
HE 220 AA	18	205	6	220	8.5
HE 240 AA	21	224	6.5	240	9
HE 260 AA	24	244	6.5	260	9.5
HE 280 AA	24	264	7	280	10
HE 300 AA	27	283	7.5	300	10.5
HE 320 AA	27	301	8	300	11
HE 340 AA	27	320	8.5	300	11.5
HE 360 AA	27	339	9	300	12
HE 400 AA	27	378	9.5	300	13
HE 450 AA	27	425	10	300	13.5
HE 450 A	27	440	11.5	300	21
HE 500 AA	27	472	10.5	300	14
HE 500 A	27	490	12	300	23
HE 550 AA	27	522	11.5	300	15
HE 550 A	27	540	12.5	300	24
HE 550 B	27	550	15	300	29
HE 600 AA	27	571	12	300	15.5
HE 600 A	27	590	13	300	25
HE 600 B	27	600	15.5	300	30
HE 650 AA	27	620	12.5	300	16
HE 650 A	27	640	13.5	300	26
HE 650 B	27	650	16	300	31
HE 700 AA	27	670	13	300	17
HE 700 A	27	690	14.5	300	27
HE 700 B	27	700	17	300	32
HE 800 AA	30	770	14	300	18
HE 800 A	30	790	15	300	28
HE 800 B	30	800	17.5	300	33
HE 800 M	30	814	21	303	40
HE 900 AA	30	870	15	300	20
HE 900 A	30	890	16	300	30
HE 900 B	30	900	18.5	300	35
HE 900 M	30	910	21	302	40
HE 900 x 391	30	922	25	307	46
HE 1000 AA	30	970	16	300	21
HE 1000 x 249	30	980	16.5	300	26
HE 1000 A	30	990	16.5	300	31
HE 1000 B	30	1000	19	300	36
HE 1000 M	30	1008	21	302	40
HE 1000 x 393	30	1016	24.4	303	43.9
HE 1000 x 415	30	1020	26	304	46
HE 1000 x 438	30	1026	26.9	305	49
IPE AA 140	7	136.6	3.8	73	5.2
IPE A 140	7	137.4	3.8	73	5.6
IPE AA 160	9	156.4	4	82	5.6
IPE A 160	9	157	4	82	5.9
IPE AA 180	9	176.4	4.3	91	6.2
IPE A 180	9	177	4.3	91	6.5
IPE AA 200	12	196.4	4.5	100	6.7
IPE A 200	12	197	4.5	100	7
IPE AA 220	12	216.4	4.7	110	7.4
IPE A 220	12	217	5	110	7.7
IPE 220	12	220	5.9	110	9.2
IPE AA 240	15	236.4	4.8	120	8
IPE A 240	15	237	5.2	120	8.3
IPE 240	15	240	6.2	120	9.8
IPE A 270	15	267	5.5	135	8.7
IPE 270	15	270	6.6	135	10.2
IPE O 270	15	274	7.5	136	12.2
IPE A 300	15	297	6.1	150	9.2
IPE 300	15	300	7.1	150	10.7
IPE O 300	15	304	8	152	12.7
IPE A 330	18	327	6.5	160	10
IPE 330	18	330	7.5	160	11.5
IPE O 330	18	334	8.5	162	13.5
IPE A 360	18	357.6	6.6	170	11.5
IPE 360	18	360	8	170	12.7
IPE O 360	18	364	9.2	172	14.7
IPE A 400	21	397	7	180	12
IPE 400	21	400	8.6	180	13.5
IPE O 400	21	404	9.7	182	15.5
IPE A 450	21	447	7.6	190	13.1
IPE 450	21	450	9.4	190	14.6
IPE O 450	21	456	11	192	17.6
IPE A 500	21	497	8.4	200	14.5
IPE 500	21	500	10.2	200	16
IPE O 500	21	506	12	202	19
IPE A 550	24	547	9	210	15.7
IPE 550	24	550	11.1	210	17.2
IPE O 550	24	556	12.7	212	20.2
IPE A 600	24	597	9.8	220	17.5
IPE 600	24	600	12	220	19
IPE O 600	24	610	15	224	24
IPE 750 x 134	17	750	12	264	15.5
IPE 750 x 147	17	753	13.2	265	17
IPE 750 x 173	17	762	14.4	267	21.6
IPE 750 x 196	17	770	15.6	268	25.4
IPE 750 x 220	17	779	16.5	266	30

Plates that can be found in real columns, or in general, compressed steel members, were studied varying the plate aspect ratio in a relevant range, see Table 2. The smallest length (L1) was taken as three times the plate width c, as defined in EN 1993-1-1 [1].

$$c = h - 2r - 2t_f \quad \text{for webs} \quad (2)$$

$$c = b/2 - r - t_w/2 \quad \text{for flanges} \quad (3)$$

The other lengths were obtained as multiples of c, with the maximum value (L6) equal to thirteen times such width. The analyses were carried out for five different temperature levels (Table 2) in the 400-800°C range, where the critical temperature of steel members typically lies [9],[13],[18]. The resistance to compression of the plates was studied considering 6 different imperfection shapes. The initial imperfection magnitude was defined according to EN 1090-2: 2008 + A1 [8] and then reduced to 80% according to the Annex C of EN1993-1-5 [2]. In total 32040 analyses were performed.

Two different numerical models representative of the web and the

flange plates were defined. Provisions for local buckling and section classification in EN 1993-1-1 [1] and EN 1993-1-5 [2] are based on the assumption of simply supported (s.s.) plates, on four sides for webs and on three sides in the case of flanges. These boundary conditions were employed in the numerical models and were considered to define 5 out of 6 imperfection shapes. Indeed, the elastic theory provides closed-form equations for the buckling modes of plates at ambient temperature assuming the aforementioned boundary conditions [23].

$$w = w_0 sin\left(\frac{m\pi x}{L}\right) sin\left(\frac{\pi y}{c}\right) \quad \text{for webs (s.s. on 4 sides)} \quad (4)$$

$$w = w_0 sin\left(\frac{m\pi x}{L}\right) sin\left(\frac{\pi y}{2c}\right) \quad \text{for flanges (s.s. on 3 sides)} \quad (5)$$

in which m is the number of half waves in the length of the plate L and w_0 is the amplitude. The number of halfwaves m is an integer number, and the value giving the critical buckling mode varies with the aspect ratio L/c. Though for flanges the critical value, i.e., the one minimising the associated buckling load, is always obtained for m=1, for webs the value of m that minimises the following equation should be found

$$\arg\min_m \left(m + \frac{1}{m}\frac{L^2}{c^2}\right)^2 \quad (6)$$

In the performed analyses, the shapes of initial geometrical imperfections were defined by considering the value m that minimises the buckling load according to the analytical solution and by increasing by 1 the number of halfwaves in 4 additional configurations, namely m+1, m+2, m+3, and m+4 (Table 2). The number of halfwaves was not decreased since preliminary analyses showed that higher resistance to compression were always found for shapes with a number of halfwaves smaller than m. A further imperfection shape was determined performing a linear buckling analysis LBA (Table 2). This procedure is usually employed in the practice to determine the buckling mode giving the lowest buckling load in a numerical model. It follows, that for the studied plates the obtained shape is essentially the same as the one determined with the analytical solution of Eq. (4) and (5). However, since the LBA method is numerical and not analytical, some small differences may be found in the initial position of the nodes, and the result may be slightly different. Nevertheless, the imperfections based on LBA were considered as the shape that would be employed in typical numerical analyses and was used as reference for the results obtained with the other shapes of imperfection.

Table 2 Parameters range

Parameter	Investigated range
Length L	L1 to L6 = [3, 5, 7, 9, 11, 13] x c
Temperature θ [°C]	[400, 500, 600, 700, 800]
Imperfection shape	[LBA, m, m+1, m+2, m+3, m+4]

Numerical analyses on compressed plates were carried out employing the triangular shell finite elements presented in [5]. Residual stresses were deemed negligible as it was shown that, owing to their relaxation with the steel temperature increase, they have no significant effects on the resistance of steel members in fire [12][17]. The temperature of the plates was kept constant at the chosen temperature level, while the compressive load was progressively increased until failure. Plates were loaded on one side with a master-slave condition that guaranteed a uniform axial displacement of the loaded side, while reaction forces were provided at the opposite side by axial restraints. Vertical restraints were applied to define the simply supported conditions on four (webs) and three sides (flanges). To prevent lateral buckling for very long plates, yet allowing for lateral expansion, additional lateral restraints were imposed at the nodes of the longitudinal midline for webs and on one side for flanges. The numerical model and the applied restraints are depicted in Figure 1. Mesh consisting of triangular grids with 8 subdivisions in the width were used, since for more subdivision it was found that the results did not significantly change. Instead, a varying number of subdivisions was chosen in the length of the plate to keep the shell aspect ratio close to 1, which is the aspect ratio allowing for the best performance and accuracy.

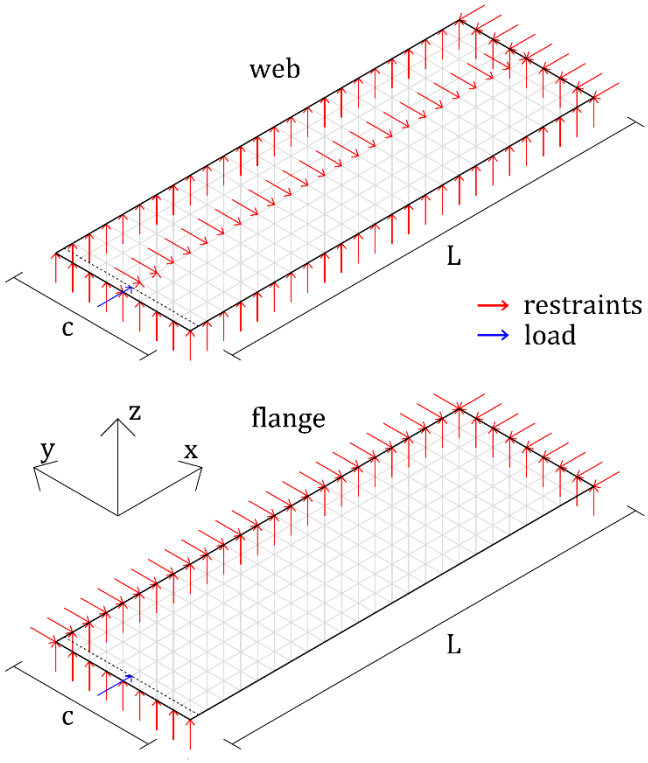

Figure 1: Numerical models for plates and webs

3 Discussion of the results

The results of numerical simulation were collected in terms of the applied axial load at failure N together with the length L, the temperature of the plate θ and the plate slenderness at elevated temperature $\lambda_{p,\theta}$, calculated as follows

$$\lambda_{p,\theta} = \frac{c/t}{28.4\varepsilon_\theta\sqrt{k_\sigma}} \quad (7)$$

with t=t_f and $k_\sigma = 0.43$ for flanges, t=t_w and $k_\sigma = 4$ for webs, and ε_θ obtained from Eq. (1). Figure 2 shows the results for web and flange plates with a uniform temperature distribution of 400°C. The axial load at failure N is normalised with respect to the yielding load N_{yield}

$$N_{yield} = Af_{y,\theta} = c \cdot t \cdot k_{y.\theta} f_y \quad (8)$$

Where A is the transversal area of the plate and $k_{y.\theta}$ is the retention factor that accounts for the reduction of the yield strength f_y at elevated temperature. For webs, failure due to buckling was always attained because of the high plate slenderness, whilst for stocky flange plates almost the full yield capacity was reached at failure ($N/N_{yield} \approx 100\%$). As expected from the elastic theory [23], significant resistance reductions were obtained due to buckling

when the plate slenderness increases, while very small failure load variations were obtained by increasing the plate length, in particular when the LBA and m imperfections were employed. In addition, it can be observed that regular surfaces are obtained for each imperfection shape for both webs and flanges, which means that the failure load N varies gradually with the length L and the slenderness $\lambda_{p,\theta}$.

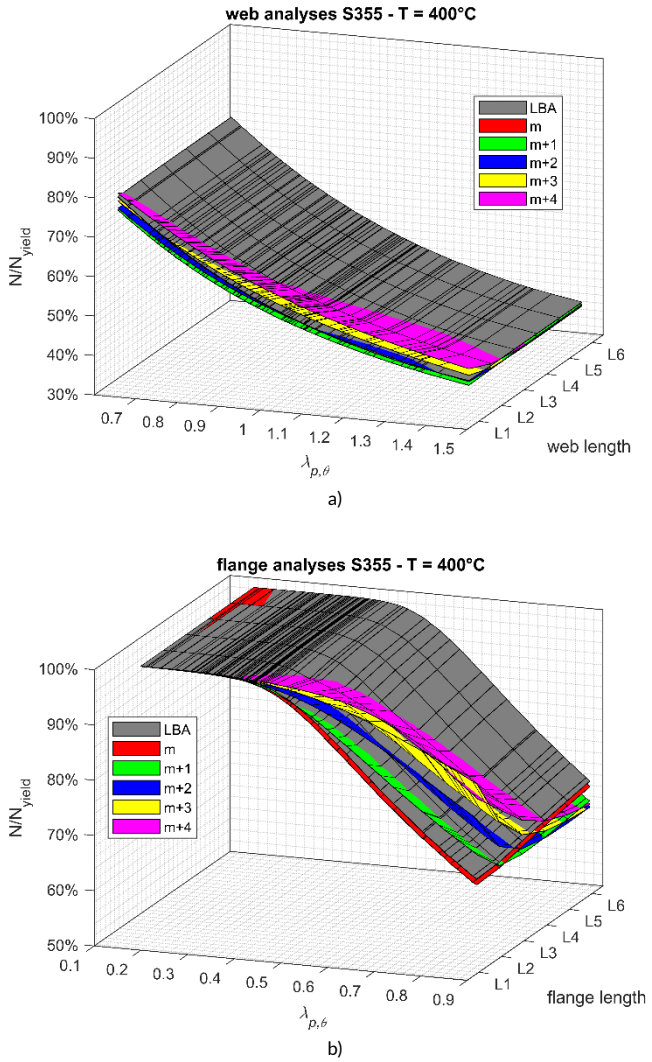

Figure 2 Failure-yielding load ratio N/N_{yield} [%] at 400°C: a) webs; b) flanges

Nevertheless, Figure 2 does not allow for a straightforward identification of the imperfection shapes that give the lowest failure loads N. Therefore, results are rearranged in Figure 3, Figure 4 and Figure 5 that report the variation of the failure load N for each imperfection shape with respect to the failure load obtained with the reference LBA imperfection N_{LBA}.

Figure 3 shows the variation of the resistance with temperature for webs (Figure 3a) and flanges (Figure 3b). Since a significant variability in the results is found at each temperature level, it appears clear that considerations based only on the temperature are not sufficient to describe the influence of the shape of imperfections on the resistance to compression. However, since the average resistance variation $(N - N_{LBA})/N_{LBA}$, reported with discontinuous lines, is not varying significantly for any imperfection shape, the retention coefficients of the mechanical properties k given in EN 1993-1-2 [3] seem adequate to account for the effects of temperatures also in this context.

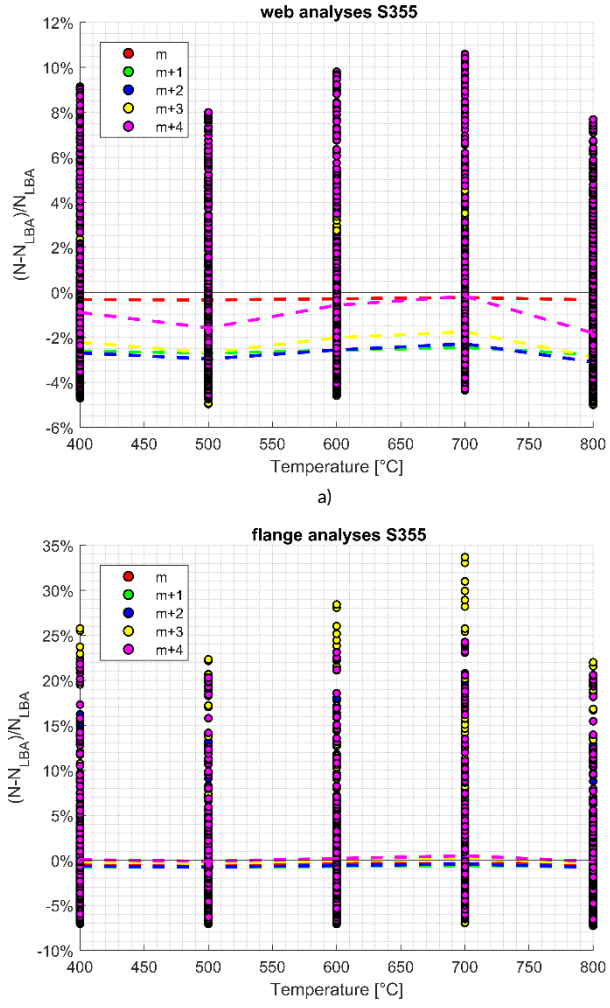

Figure 3 Variation of the failure load with temperature T: a) webs; b) flanges

More significative indications can be taken from Figure 4 and Figure 5, in which the numerical outcomes are presented with respect to the plate slenderness at elevated temperature $\lambda_{p,\theta}$ and the length of the plate L, respectively. Figure 4a highlights that for all the imperfections in which the number of halfwaves was increased (m+1 to m+4), the variation of the web resistance $(N - N_{LBA})/N_{LBA}$ always increases until a slenderness of 0.95 is reached. Interestingly, the LBA-based and m imperfections never give the lowest failure load, but it is not possible to identify a single imperfection shape that always provides the lowest failure load. In general, by increasing the number of additional halfwaves a higher dispersion of the variation of the resistance is obtained and thus, the m+4 imperfection results in being the most conservative or the most unconservative shape, depending on the case. The m+1 imperfection instead, provides failure loads that are always lower than the ones obtained from the LBA imperfection, as also confirmed in [16], but rarely provide the absolute lowest failure load. Figure 4b shows that also for the flanges there is no shape of imperfection that always gives the lowest failure load. Moreover, all the imperfections with a number of halfwaves higher than m may entail failure loads higher than N_{LBA}. More consistent variations are found compared to the web plates analyses for $\lambda_{p,\theta}$>0.5.

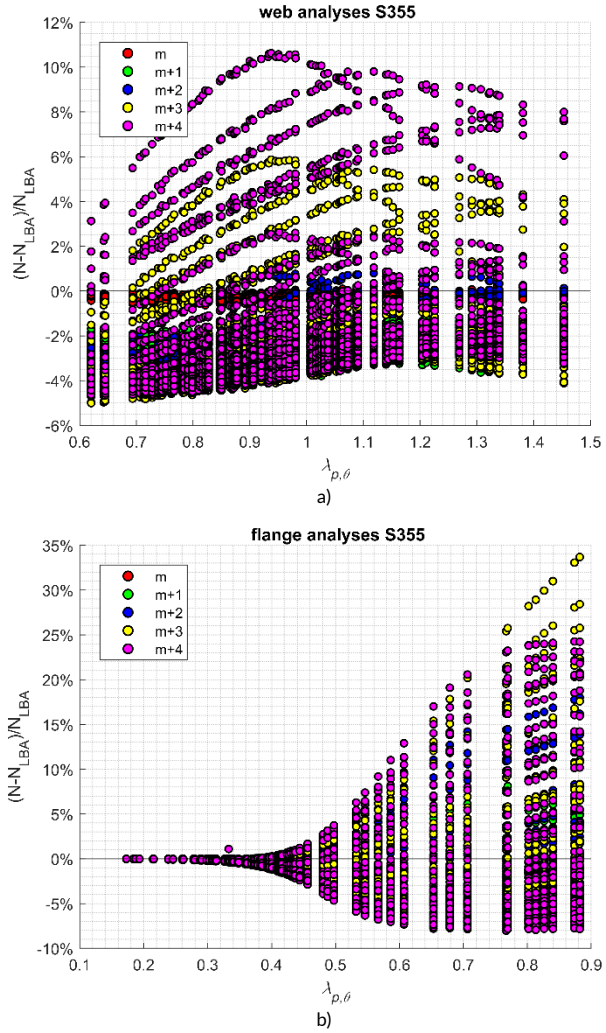

Figure 4 Variation of the failure load with the plate slenderness $\lambda_{p,\theta}$: a) webs; b) flanges

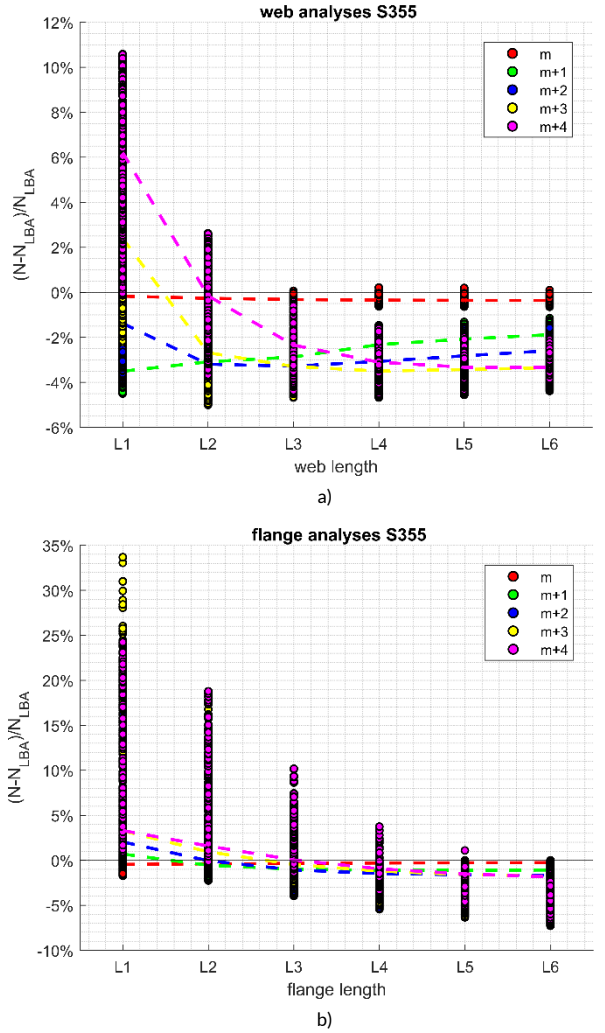

Figure 5 Variation of the failure load with length of the plate L: a) webs; b) flanges

Figure 5 highlights that the variation of the failure load of a given imperfection shape with respect to N_{LBA} depends on the length of the plate. The lowest average variations for webs, i.e., the minimum values assumed by the discontinuous lines in Figure 5a, are always between -3% and -4%, though they are associated to different imperfection shapes depending on the length L. For webs with a small aspect ratio L/c the lowest average failure loads are obtained with the m+1 imperfection, but increasing the length imperfections with a higher number of halfwaves become critical and for L5 and L6 the lowest average failure load is attained with the m+4 imperfection. Similar observations can be taken for flanges from Figure 5b. However, it should be noted that while imperfections with a number of halfwaves higher than m are always critical for webs, for very small aspect ratio L1, i.e., L/c =3, the lowest average failure load is obtained with the imperfection designed with m halfwaves.

Two general considerations can be taken observing Figure 3 to Figure 5. The results obtained with the LBA-based and the m imperfections are essentially the same, since the difference between the two failure loads is almost constant and negligible in all the figures. This confirms that the numerical model is adequate to study simply supported plates as reported in the literature [23] and that the elastic buckling modes are correctly identified when LBA is used. In addition, it can be observed that the resistance varies in a small range for webs (about -5% to +11%), while the resistance of flanges varies in a larger range (about -8% to +34%).

4 Conclusions

In this paper the influence of different shapes of the initial imperfection on the resistance of compressed steel webs and flanges at elevated temperatures was studied. It was observed that the imperfection shapes suggested by the elastic theory of plates m, or by a linear buckling analysis LBA do not always provide the lowest failure load. Four additional sinusoidal shapes were defined increasing the number of halfwaves from m to m+4. It was shown that the imperfection shape giving the lowest failure load varies with both the length and the slenderness at elevated temperature of the web and flange plates. For very small aspect ratio L/c, increasing the number of halfwaves might be detrimental, especially for flange plates. Instead, when the plate length is increased, shapes with a number of halfwaves bigger than m allow for failure loads lower than the ones obtained with the LBA-based and the m imperfections. Nevertheless, when m+1 to m+4 imperfections were used a 10% reduction of the failure load was never attained, while significant overestimations of about 34% were obtained in some cases. Thus, the employment of LBA is still suggested since it allows for predictions that do not significantly overestimate the lowest failure load. However, for more conservative results, the m+1 imperfection can be employed for web analyses, as it always provided failure loads lower than N_{LBA} and N_m. For flanges, the LBA-based or m imperfections should be used for $\lambda_{p,\theta}$<0.5 and L\c<7, while the number of halfwaves could be increased otherwise. In detail, for $\lambda_{p,\theta}$≥0.5 the lowest failure load is usually found for m+1 and L\c=7, m+2 and L\c=9, m+3 and L\c=11 and m+4 and L\c=13.Further

studies are expected, in order to investigate different aspects, like the influence of the steel grade or the imperfection magnitude, and to understand if similar findings apply to full steel sections as well.

Acknowledgements

The support received from the Italian Ministry of Education, University and Research (MIUR) in the frame of the 'Departments of Excellence' (grant L 232/2016) is gratefully acknowledged.

References

[1] European Committee for Standardisation (2005). *Eurocode 3 Design of steel structures - Part 1-1: General rules and rules for buildings.*

[2] European Committee for Standardisation (2006). *Eurocode 3 Design of steel structures - Part 1-5: Plated structural elements.*

[3] European Committee for Standardisation (2005). *Eurocode 3 Design of steel structures - Part 1-2: General rules - Structural fire design.*

[4] Wagner W. and P. Wriggers (1988), *Simple method for the calculation of postcritical branches*, Eng. Comput., **5**(2), pp- 103–109

[5] L. Possidente, N. Tondini, J.-M. Battini (2018). *Branch-switching procedure for post-buckling analyses of thin-walled steel members in fire*. Thin-Walled Structures **136**, pp. 90-98.

[6] European Committee for Standardisation (1993). *EN 10034: Structural steel I and H sections – Tolerances on shape and dimensions.*

[7] European Committee for Standardisation (2008). *EN 1090-2: Execution of steel structures and aluminium structures - Part 2 :Technical requirements for steel structures.*

[8] European Committee for Standardisation (2011). *EN 1090-2: 2008 + A1 Execution of steel structures and aluminium structures - Part 2 : Technical requirements for steel structures*

[9] J.-M. Franssen, J.-B. Schleich, L.-G. Cajot (1995). A simple Model for the Fire Resistance of Axially-loaded Members According to Eurocode 3. Journal of Constructional Steel Research, **35**, pp. 49-69.

[10] J.-M. Franssen, J.-B. Schleich, L.-G. Cajot, W. Azpiazu (1996). A simple Model for the Fire Resistance of Axially-loaded Members Comparison with Experimental Results. Journal of Constructional Steel Research, **37**, pp. 175-204.

[11] M. Knobloch, M. Fontana (2006). *Strain-based approach to local buckling of steel sections subjected to fire*. J. Construct. Steel Res., **62**, pp. 44–67.

[12] C. Couto, P. Vila Real, N. Lopes, B. Zhao (2014), *Effective width method to account for the local buckling of steel thin plates at elevated temperatures.* Thin-Walled Struct., **84** pp. 134–149.

[13] C. Couto, P. Vila Real, N. Lopes, B. Zhao (2015), *Resistance of steel cross-sections with local buckling at elevated temperatures*. J. Construct. Steel Res., **109**, pp. 101-114.

[14] C. Couto, P. Vila Real, N. Lopes, B. Zhao (2016), *Local buckling in laterally restrained steel beam-columns in case of fire*. J. Construct. Steel Res., **122**, pp. 543-556.

[15] C. Maraveas, T. Gernay, J.-Marc Franssen (2017). *Sensitivity of elevated temperature load carrying capacity of thin-walled steel members to local imperfections*. Proceedings of ASFE 2017 Conference, 7 September; Manchester, UK

[16] C. Maraveas, T. Gernay, J.-Marc Franssen (2017). *Buckling of steel plates at elevated temperatures: theory of perfect plates vs finite element analysis.* CONFAB 2017, 10-12 September; London, UK

[17] S. E. Quiel, M. E. M. Garlock (2010), *Calculating the buckling strength of steel plates exposed to fire*. Thin-Walled Structures **48**, No. 9, pp. 684-695

[18] G. C. Calobrezi, V. Pignatta Silva (2020). On the Local Buckling of Steel "I" Profiles in a Fire Situation, Fire Technology **57**, pp. 415–438

[19] C. Couto, P. Vila Real, N. Lopes, B. Zhao (2016), *Numerical investigation of the lateral-torsional buckling of beams with slender cross section for the case of fire*. Engineering Structures, **106**, pp. 410-421.

[20] M. Prachar, J. Hricak, M. Jandera, F. Wald, B. Zhao (2016). *Experiments of Class 4 open section beams at elevated temperatures*. Thin-Walled Structures, **98**, pp. 2-18

[21] J.-M. Franssen, F. Morente, P. Vila Real, F. Wald, A. Sanzel, B. Zhao (2016). *Fire Design of Steel Members with Welded or Hot-rolled Class 4 Cross-sections (FIDESC4).*

[22] C. Couto, P. Vila Real, (2021), *The influence of imperfections in the critical temperature of I-section steel members*. J. Construct. Steel Res, **179**.

[23] S. P. Timoshenko, J. M. Gere (1961). Theory of Elastic Stability, McGraw-Hill, New York